

# Analysis of the Effects of Overcharging Lithium Ion Cells with Graphite Anode: Efficiency of Protection Devices Integrated into the Cells

Carla Menale<sup>a</sup>, Francesco Vitiello<sup>a,\*</sup>, Antonio Nicolò Mancino<sup>a</sup>, Vincenzo Sglavo<sup>a</sup>, Francesco Vellucci<sup>a</sup>, Antonio Scotini<sup>b</sup>

<sup>a</sup> Laboratorio Mobilità Sostenibile e Trasporti, ENEA, Via Anguillarese 301, 00123, Roma, Italia.

<sup>b</sup> Laboratorio Idrogeno e nuovi Vettori Energetici, ENEA, Via Anguillarese 301, 00123, Roma, Italia.

[francesco.vitiello@enea.it](mailto:francesco.vitiello@enea.it)

Lithium ion batteries are currently the main technology for storing energy in electric vehicles thanks to their high power density and energy density. Among the many challenges, safety related aspects must be faced. The thermal runaway caused by overcharge is one of the main weak points to be addressed to ensure a proper level of safety, necessary for the diffusion of this technology. Nowadays, many cells have integrated protection devices that reduce the risk of thermal runaway triggered by overcharging. In this study, the efficiency of devices used to prevent the thermal runaway, caused by overcharging cylindrical 18650 lithium-ion cells with graphite anode, is evaluated. Experimental tests were carried out at different ambient temperatures and overcharge currents. In all the cases the intervention of the Current Interrupt Device avoids the thermal runaway occurrence, preventing the intervention of the others protection devices such as the Positive Temperature Coefficient device and the safety vent.

## 1. Introduction

In recent decades lithium ion batteries (LIBs) rapidly spread due to their high power density, high energy density and long cycle life. In addition to consumer electronics, where these cells are widely used, the boost in decarbonization of transport and, in general, of energy production and distribution, pushes them to face major challenges as energy storage system for electrified vehicles and for stationary storage systems. As any technology, LIBs have weaknesses: whenever the batteries work outside of their narrow operating temperature range or outside the charge/discharge rate and voltage limits they suffer from rapid degradation, and, in case of severe abuse, Thermal Runaway (TR) can occur with consequent ignition of the surrounding material.

The Thermal Runaway is a chain reaction of uncontrollable and irreversible battery temperature and internal pressure increase that develops inside the cells and that can lead to gas leakage, fire and explosion. The different types of abuse, mechanical, electrical and thermal, can lead to the failure of the separator causing an Internal Short Circuit (ISC) within the battery. Tran et al (2022) summarize the Thermal Runaway temperature response as characterized by three temperatures.  $T_1$  is the onset temperature, at which the battery experiences self-heating, caused by solid electrolyte interface (SEI) decomposition.  $T_2$  is the Thermal Runaway trigger temperature caused by separator failure that leads to an ISC; at this point the temperature rise from a constant to a quasi-exponential curve.  $T_3$  is the highest temperature. According to Feng et al. (2018), for the Thermal Runaway caused by overcharge the generated heat is proportional to the overcharge current intensity. In case of low current, swelling of the cell can occur, while in case of high current the cell might explode.

For the above mentioned reasons, some cells are equipped with safety devices. These can include Current Interrupt Device (CID), safety vent and Positive Temperature Coefficient (PTC) device. The CID and the safety vent are both activated by pressure. When the CID activation pressure is reached the device cut off the electrical pathway from the current collector to the external load, halting the electrochemical reaction. If the pressure continues to build up the safety vent mechanism activates. The PTC is an electrode whose resistance rises

sharply when the temperature goes above his response threshold. It often consists of a polymer containing conductive particles that complete the circuit between the cathode and the positive connector of the cell. At normal operation temperature it maintains its conductive state, while it becomes an insulator at temperature over its response threshold.

Two test campaign, Li et al. (2020) and Li et al. (2022), measured the activation pressure of CID and safety vent at ambient temperature (22 °C) and high temperature (100 °C) on four brands of 18650 cells, achieving lower activation pressure with temperature increase for both the protection devices in all cell types tested. The CID activation pressure was approximately 1 MPa while safety vent activation pressure was approximately 2 MPa. They also performed several simulations to estimate the activation pressure at very high temperatures (300 °C) confirming the reduction trend also with very high temperature.

Meng et al. (2023) performed thermal runaway tests on a 18650 cell measuring a temperature of the external cell case of 117.9 °C at the moment of current interruption due to PTC. The charge rate was 0.5C. For charge rate of 3C the current interruption occurred at lower temperature: 82.3 °C.

In the following sections are presented the results of overcharge abuse test performed on 18650 cells with graphite based anode, equipped with all the three safety device described before (CID, safety vent and PTC). In the next section is described the set up used, while in the following paragraphs the results and the conclusions are reported.

## 2. Experimental setup

The overcurrent abuse tests were carried out in a climatic chamber containing an experimental set-up that houses the cell, shown in Figure 1. The purpose of this set up is to avoid the dispersion of the mechanical parts and to contain the gases in the event of activation of the safety vent or, in the worst case scenario, of the explosion of the cell. The set up consists of a container, whose design is based on literature data related to the gas amount produced during venting and the consequent overpressure generated, and it is equipped with a pressure transducer to measure, in real time, a pressure increase. A pressure increase would detect a possible release of gas from the cell, due to venting or breaking/explosion. The set up is equipped with a drain valve to draw off the possible venting gases and a safety valve that intervenes whenever the pressure goes over the maximum value allowed by the transducer.

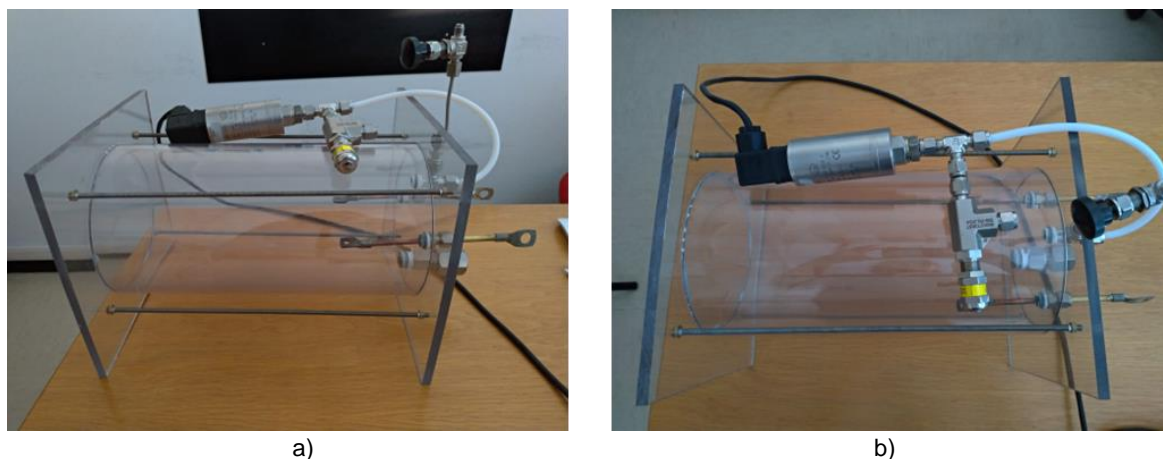


Figure 1: Cell container: a) lateral view, b) top view.

The cells under test were 18650 cell type with graphite-based anode (NCR18650B), whose main characteristics are shown in Table 1.

The cell monitoring is performed with:

- 3 calibrated thermocouples, type K (accuracy of  $\pm 0.1$  °C) located close to the positive connector, at cell center and close to the negative connector;
- a National Instrument "CompactDAQ" chassis with a thermocouple module (24 bit ADC, 16 channels) and one voltage input module (16 bit ADC, 32 channels);
- a data acquisition system designed by using LabVIEW.

Table 1: Characteristics of the tested cells

|                     | NCR18650B         |
|---------------------|-------------------|
| Rated Capacity      | 3200 mAh          |
| Nominal Voltage     | 3.6 V             |
| Max. Charge Voltage | 4.2 V             |
| Standard Charge     | 1625 mA (0.5C)    |
| Charge Temp. Range  | 0 °C to +45 °C    |
| Dimension (DxH)     | 18.5 mm x 65.3 mm |
| Weight              | 46.5 g            |

Each cell was subjected to preliminary standard charge/discharge cycles with an Eltra E-8094 cyler (nominal voltage 3.6 ÷ 6 V, current 0 ÷ 280 A), whereas the abuse tests were performed with a portable Eltra E-8325 cyler (voltage 0 ÷ 18 V, maximum charge current 80 A and maximum discharge current 150 A). Using the cyler made it possible to acquire the data related to the state of the battery and to identify the SOC % reached at the end of overcharge. A total of eight cells were tested, seven with a current of 3C (9.6 A) and one with a current of 1C (3.2 A). The ambient temperature varied from 20 °C to 50 °C by means of the climatic chamber. The Figure 2 shows the climatic chamber with the set up that houses the cell under test.



Figure 2: Climatic Chamber with cell container.

### 3. Results and discussion

The results obtained in the overcharge tests are summarized in Table 2. The occurrence of thermal runaway, venting phenomena, fire or explosion, was not observed in any test as confirmed by the absence of significant variation of the container pressure measured during each test. The State of Charge (SOC) in Table 2 is related to the moment when the cyler stops supplying the constant current of 9,6 A or 3,2 A. The overcharge duration is the time interval during which a constant current of 9,6 or 3,2 is applied, and the maximum temperature is related only to the same period.

Table 2: Summary of the results obtained from the overcharge tests

| Cell number | Overcharge current | Initial temperature (T <sub>0</sub> ) | Duration of the overcharge | Maximum temperature (T <sub>max</sub> ) | $\Delta T = T_{max} - T_0$ | SOC % |
|-------------|--------------------|---------------------------------------|----------------------------|---|----------------------------|-------|
| 1           | 9.6 A              | 20 °C                                 | 338 s                      | 72.3 °C                                 | 52.3 °C                    | 127   |
| 2           | 9.6 A              | 30 °C                                 | 279.4 s                    | 70.6 °C                                 | 40.6 °C                    | 123   |
| 3           | 9.6 A              | 40 °C                                 | 302.1 s                    | 80.9 °C                                 | 40.9 °C                    | 125   |
| 4           | 9.6 A              | 40 °C                                 | 252 s                      | 72.6 °C                                 | 32.6 °C                    | 121   |
| 5           | 3.2A               | 50 °C                                 | 993.7 s                    | 73.9 °C                                 | 23.9 °C                    | 127   |
| 6           | 9.6 A              | 50 °C                                 | 192.3 s                    | 72 °C                                   | 22 °C                      | 116   |
| 7           | 9.6 A              | 50 °C                                 | 175.6 s                    | 70.5 °C                                 | 20.5 °C                    | 114   |
| 8           | 9.6 A              | 50 °C                                 | 169.6 s                    | 71 °C                                   | 21 °C                      | 114   |

In all the tests, the thermocouples close to the positive terminal always reach the highest temperature during the overcharge. This is caused by the presence of the protection devices, namely Current Interruption Device (CID) and Positive Temperature Coefficient (PTC), that, dissipate electrical energy accordingly to the previous test campaign performed by Menale et al. (2021). The Figures from 3 to 5 show the temperature trends, during and after the overcharge considering different initial temperature of 20 °C, 30 °C and 40 °C, together with the current and voltage applied. When the temperatures reach about 70°C the CID cuts off the electrical circuit stopping the overcharge. These temperatures are all within a range of 10°C, which is consistent with the variability of the process found in the previous test campaign carried out in open air with similar initial temperature by Menale et al. (2021).

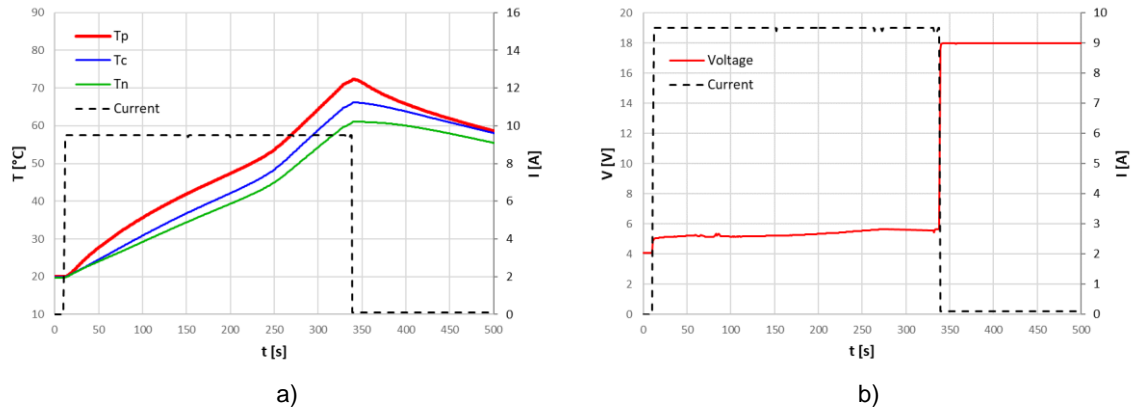


Figure 3: Overcharge with current of 9.6 A at 20 °C initial temperature: a) temperature close to: positive terminal ( $T_p$ ), cell centre ( $T_c$ ), cell negative terminal ( $T_n$ ), b) Voltage (V) and Current (I).

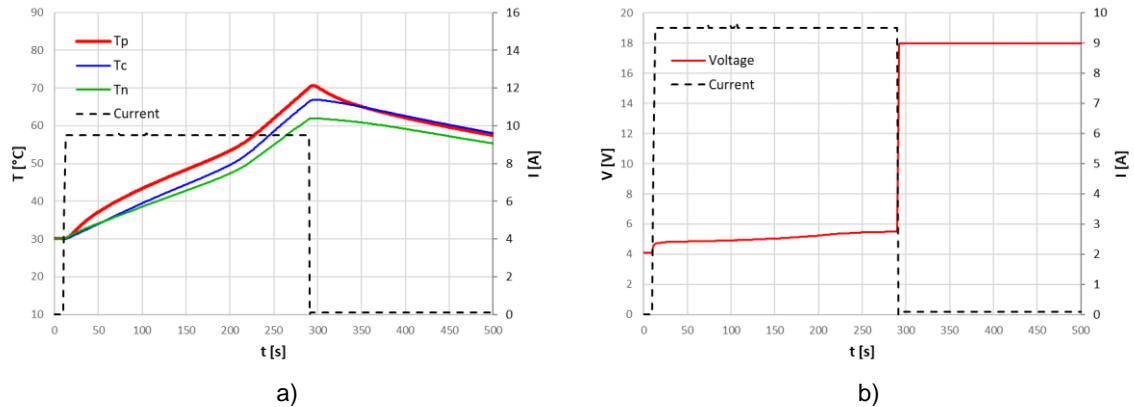


Figure 4: Overcharge with current of 9.6 A at 30 °C initial temperature: a) temperature close to: positive terminal ( $T_p$ ), cell centre ( $T_c$ ), cell negative terminal ( $T_n$ ), b) Voltage (V) and Current (I).

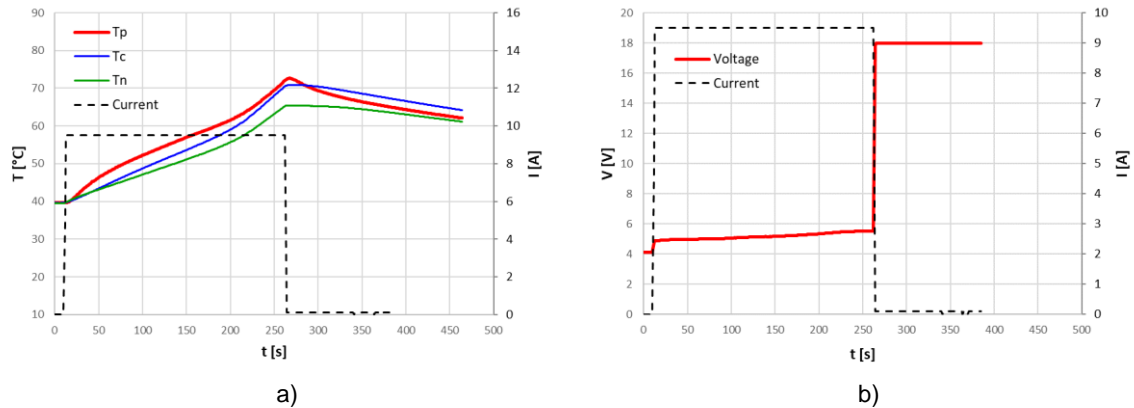


Figure 5: Overcharge with current of 9.6 A at 40 °C initial temperature: a) temperature close to: positive terminal ( $T_p$ ), cell centre ( $T_c$ ), cell negative terminal ( $T_n$ ), b) Voltage (V) and Current (I).

In this study, when the CID cuts off the electrical circuit the voltage of the cyclor reaches its saturation value of 18V, however the cells voltage measured after the test is 0, confirming the assumption of open circuit. A different behavior was observed for the tests with ambient temperature of 50 °C, as shown in Figure 6. In these cases, when the temperature reaches about 70 °C the current decreases, but the temperature continues to increase reaching a value of 87 °C after 1300 seconds. The temperature decreases only when the cyclor is turned off. This behavior is caused by a small current that flows inside the cell heating it when the cyclor voltage saturates at 18 V. Even though the cells remain in a safe state, this test highlights the CID triggering failure for ambient temperature above 50 °C, pointing out that a small current can involve an important increase in the temperature of abused cells.

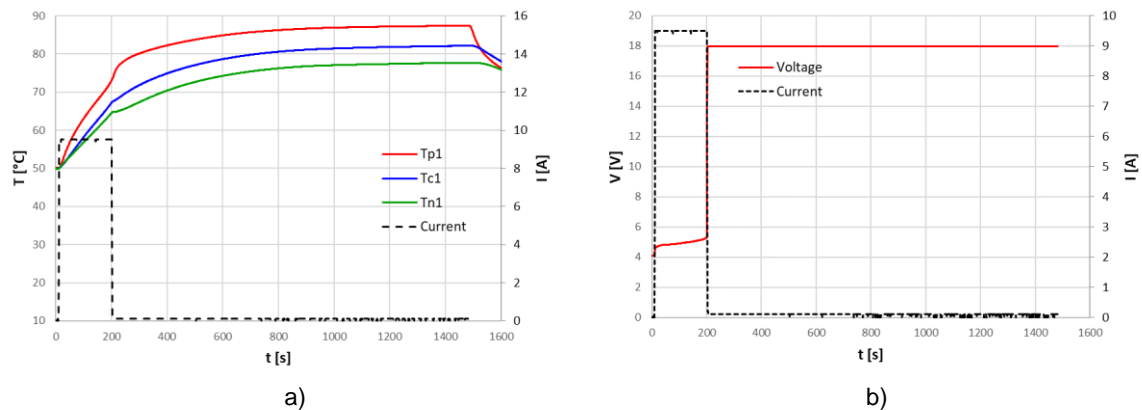


Figure 6: Overcharge with current of 9.6 A at 50°C initial temperature: a) temperature close to: positive terminal ( $T_p$ ), cell centre ( $T_c$ ), cell negative terminal ( $T_n$ ), b) Voltage ( $V$ ) and Current ( $I$ ).

The Figure 7 shows a comparison for each ambient temperature of the voltage and the SOC reached at the CID intervention, that occurs when the voltage rises sharply towards the saturation value, 18 V. The final SOC decreases as the ambient temperature increases: at 20 °C ambient temperature a SOC of 127% is obtained, while at 50 °C ambient temperature a SOC of 114% is obtained. The same trend is observed increasing the overcharge current: with a fixed ambient temperature of 50 °C, supplying a current of 3.2 A a SOC of 127% is obtained while supplying a current of 9.6 A a SOC of 114% is obtained. With an increase of the ambient temperature the voltage reached before the CID intervention also decreases.

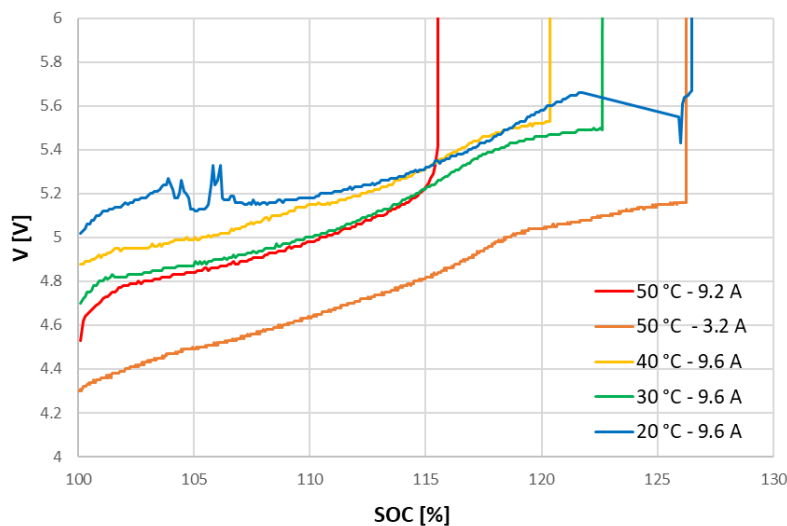


Figure 7: Comparison of the voltage ( $V$ ) and SOC reached at CID triggering.

#### 4. Conclusions

In this work, a campaign of overcharge abuse tests was carried out to verify the effectiveness of protection devices embedded in lithium ion cylindrical cells. The tests were performed at different currents and ambient temperatures, inside a climatic chamber. An experimental set up was created to avoid material and gas dispersion inside the climatic chamber and to detect the cell venting or explosion. In all cases, no venting or thermal runaway were observed. For ambient temperatures below 50 °C the CID activated correctly, cutting off the current and thus blocking further increase in cell temperature. For an ambient temperature of 50°C, however, the flow of a small current entailed the incorrect activation of the CID. This small current led to a rise in the cell temperature from about 70 °C, the temperature when the CID activates, towards a plateau value of 87°C.

A temperature of 50 °C can be easily reached inside the battery pack if the vehicle remains parked under the sun during a warm season, an occurrence of overcharge in this condition could be critical since a small current that continues to flow in the battery, as observed in the tests, brings a considerable temperature rise.

#### Acknowledgments

The authors are grateful to the Italian Ministry of Environment and Energetic Security and ENEA for their financial support.

#### References

- Feng X., Ouyang M., Liu X., Lu L., Xia Y., He X., 2019, Thermal runaway mechanism of lithium ion battery for electric vehicles: A review, *Energy Storage Materials*, 10, 246-267, [dx.doi.org/10.1016/j.ensm.2017.05.013](https://doi.org/10.1016/j.ensm.2017.05.013).
- Li W., Crompton K.R., Hacker C., Ostaneck J. K., 2020, Comparison of Current Interrupt Device and Vent Design for 18650 Format Lithium-ion Battery Caps, *Journal of Energy Storage*, 32, 101890, [doi.org/10.1016/j.est.2020.101890](https://doi.org/10.1016/j.est.2020.101890).
- Li W., Crompton K.R., Ostaneck J. K., 2022, Comparison of current interrupt device and vent design for 18650 format lithium-ion battery caps: New findings, *Journal of Energy Storage*, 46, 103841, [doi.org/10.1016/j.est.2021.103841](https://doi.org/10.1016/j.est.2021.103841).
- Menale C., Costà S., D'Annibale F., Scotini A., Sglavo V., 2021, Experimental investigation of the overcharge effects on commercial Li-Ion Batteries with two different anode materials, *Chemical Engineering Transaction*, 86, [doi.org/10.3303/CET2186077](https://doi.org/10.3303/CET2186077).
- Meng D., Wang X., Chen M., Wang J., 2023, Effects of environmental temperature on the thermal runaway of lithium-ion batteries during charging process, *Journal of Loss Prevention in the Process Industries*, 83, 105084, [doi.org/10.1016/j.jlp.2023.105084](https://doi.org/10.1016/j.jlp.2023.105084).
- Tran M.-K., Mevawalla A., Aziz A., Panchal S., Xie Y., Fowler M. A., 2022, A Review of Lithium-Ion Battery Thermal Runaway Modeling and Diagnosis Approaches. *Processes* 2022, 10, 1192, [doi.org/10.3390/pr10061192](https://doi.org/10.3390/pr10061192).